ACS APPLIED MATERIALS & INTERFACES

Research Article

www.acsami.org

Magnetically Enhanced Bicelles Delivering Switchable Anisotropy in Optical Gels

Marianne Liebi,[†] Simon Kuster,[†] Joachim Kohlbrecher,[‡] Takashi Ishikawa,[¶] Peter Fischer,*[,†] Peter Walde,[∥] and Erich J. Windhab[†]

[†]Laboratory of Food Process Engineering, ETH Zurich, Schmelzbergstrasse 9, 8092 Zurich, Switzerland

[‡]Laboratory for Neutron Scattering, Paul Scherrer Institute, 5232 Villigen PSI, Switzerland

[¶]Biomolecular Research Laboratory, Paul Scherrer Institute, 5232 Villigen PSI, Switzerland

[∥]Department of Materials, ETH Zurich, Wolfgang-Pauli-Strasse 10, 8093 Zurich, Switzerland

ABSTRACT: Mesostructures responding to external triggers such as temperature, pH, or magnetic field have the potential to be used as self-acting sensors, detectors, or switches. Key features are a strong and well-defined response to the external trigger. Here, we present magnetic alignable bicelles embedded into a gelatin matrix generating magnetically switchable structures, which can reversibly be locked and unlocked by adjusting the temperature. We show that the disk-like aggregates can be orientated in magnetic fields, and such orientation can be preserved after embedding into gelatin. The resulting gel cubes show an anisotropic transfer for electromagnetic waves, i.e., a different spatial birefringence. Cycling through the melting point of gelatin sets the structure back to its isotropic state providing a read-out of the thermal history. Stacking of the bicelles induced by the gelatin promotes magnetic aligning, as an increased aggregation number in the stacks increases the magnetic orientation energy.

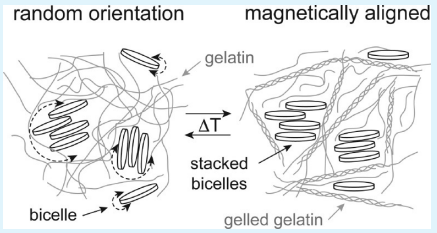

KEYWORDS: *bicelles, hydrogel, gelatin, magnetic aligning, smart material, phospholipids*

INTRODUCTION

Smart hydrogels convey the property to respond actively to a specific external stimulus. They have gained increasing interest in recent years with potential applications in controlled drug delivery, tissue engineering, sensors, microfluidic devices, and photonic applications. As possible external triggers, temperature, pH change, ionic strength, light, biomolecules (e.g., glucose), and electric and magnetic fields were investigated and reviewed.[1−5] The response can be either originated by the gel matrix itself, such as thermo- or pH sensitive hydrogels, or conferred by a functional ingredient embedded into the matrix. In either case, the response has to be clearly linked to the trigger for a successful application of a smart hydrogel.

A magnetic response is in most cases induced by the inclusion of magnetic nanoparticles into a gel matrix. Thus, the magnetic field response includes remote heating, opening and closure of pores, swelling, shrinking, and bending behavior induced by the superparamagnetic particles.[1,3,4,6−9] There are also examples using a gel matrix to preserve magnetic induced structure. In this way, magnetic aligned single-walled carbon nanotubes have been fixed with gelatin, in order to produce anisotropic composite films.[10] Christianen et al. used gelatin to fix the alignment of cyanine dye J-aggregates,[11] and magnetically deformed capsules have been fixed with an organogel, thereby keeping its oblate shape outside a magnetic field.[12]

We used magnetically aligned bicelles based on phospholipids as building blocks within a gelatin matrix to generate magnetically and thermally switchable anisotropic structures with different spatial optical properties, which can be used as smart detectors or switches. A sensor detecting the exceedance of temperature over a critical value, which coincides with the sol−gel temperature of the matrix, by the loss of the magnetic preorientation is one potential application.

Bicelles based on phospholipids are nanometer-sized aggregates. The alignment of such bicelles in a magnetic field is due to the anisotropy of the diamagnetic susceptibility $\Delta\chi$ of the phospholipids, resulting in a preferred orientation of the molecules in the magnetic field. In addition, the magnetic orientation direction of the bilayer can be selected with the use of different types of lanthanide ions complexed to the phospholipid (i.e., Tm^{3+} for a parallel aligning of the bicellar normal and Dy^{3+} for a perpendicular aligning).[13,14] In this way, the diamagnetic susceptibility $\Delta\chi$ of the phospholipids assembled in the bicelle can be enhanced by the diamagnetic susceptibility $\Delta\chi$ of the lanthanides and will result in a pronounced magnetic alignment of the bicelles subjected to an external magnetic field.[15−18] The bicelles studied here are based on mixtures from DMPC (1,2-dimyristoyl-*sn*-glycero-3-phosphocholine), cholesterol, and a chelator-lipid, DMPE-DTPA (1,2-dimyristoyl-*sn*-glycero-3-phosphoethanolamine-diethylenetriaminepentaacetate), with complexed lanthanide ions and embedded in 5%(w/w) gelatin. Whereas the bilayer forming

Received: October 21, 2013
Accepted: December 26, 2013
Published: December 26, 2013

phospholipid, i.e., DMPC, is supposed to be found mainly in the planar part of the disk, DMPE-DTPA/lanthanide with its large headgroup is assumed to cover the highly curved bilayer edges.[15] Cholesterol was reported to help integrate a larger fraction of the chelator-lipid into the plane of the disk thereby increasing the disk size and the magnetic alignability.[16] Such bicelles undergo structural changes with temperature, which are related to the phase transition temperature T_m of the phospholipid. Disk-shaped aggregates with the most pronounced aligning properties have been found at temperatures below T_m.[16] In order to optimize the degree of aligning in the gelatin-bicelles system, T_m of the phospholipid should preferentially lie above the gelation temperature of gelatin. Hence, in this study, the fatty acid tail myristoyl was replaced by palmitoyl in the bicellar mixture, i.e., DMPC (T_m = 23.6 °C)[19] by DPPC (T_m = 41.3 °C)[19] and DMPE-DTPA by DPPE-DTPA. The interaction of the optimized bicelles with the surrounding gelatin matrix can be considered as classically thermodynamically driven depletion of the polymer molecules in the vicinity of particulated aggregates, thus, the bicelles.[20] As a result of depletion, clustering of the bicelles and microscopic phase separation leads presumably to the stacking of the bicelles, which can also be seen as localized nematic arrangements embedded in gelatin.

MATERIALS AND METHODS

Materials. The phospholipids, 1,2-dipalmitoyl-*sn*-glycero-3-phosphocholine (DPPC), and DPPE (1,2-dipalmitoyl-*sn*-glycero-3-phosphoethanolamine) were purchased as a chloroform solution from Avanti Polar Lipids (Alabaster, AL) and used without further purification. Gelatin from porcine skin (approximately 300 bloom, Type A BioReagent powder), $TmCl_3$ (99.9%), $DyCl_3$ (99.9%), cholesterol (99%), D_2O (99.9 atom % D), and methanol (99.8%) were from Sigma-Aldrich (Buchs, Switzerland); chloroform (stabilized with EtOH) was from Ecsa (Balerna, Switzerland). Stock solutions of 10 mM $TmCl_3$ in MeOH and of 10 mM cholesterol in chloroform were prepared.

Synthesis of DPPE-DTPA. The synthesis of DPPE-DTPA followed an adopted recipe of Aikawa et al.[21] Under inert atmosphere, diethylenetriaminepentaacetic acid dianhydride (2.16 g, 14.45 mmol, 5 equiv) was mixed in DMF absolute over MS 4 Å (150 mL) and trietylamine (4.03 mL, 2.92 g, 28.9 mmol, 10 equiv) freshly distilled over calcium hydride. The mixture was heated to 50 °C and stirred for 1 h until everything was dissolved. A second solution was prepared under inert atmosphere of DPPE (2 g, 2.89 mmol, 1 equiv) in freshly distilled chloroform (25 mL) over calcium hydride. This solution was then dropwise added to the first one within 20 min. The reaction mixture was stirred at 50 °C for an additional 2 h before the reaction was quenched by the addition of water (5 mL). The solvent of the reaction mixture was removed at the rotary evaporator under reduced pressure. A small amount of aqueous hydrochloric acid (1 M, 20 mL) was added prior to extracting the product with a solution of chloroform and methanol (5/1, 200 mL). The solvent combined with the Na_2SO_4 dried organic layer was removed under reduced pressure, and the residue was recrystallized in acetonitrile (50 mL). Subsequent purification by silica column chromatography (chloroform/methanol/water/formic acid = 65:25:40:10) of the crude product yielded DPPE-DTPA (0.42 g, 0.39 mmol, 14%) as light gray powder. HR-MS: calculated for $C_{51}H_{96}N_4O_{17}P$ $[M + H]^+$: 1067.6503; found: 1067.6497. $\Delta m/z$: 0.56 ppm.

Preparation of Bicelles and Gelatin Solution. Bicelles were produced as described previously by thin film hydration.[15,16] Molar ratio of DPPC/cholesterol/DPPE-DTPA/Tm^{3+} was 16:4:5:5, and total lipid concentration was 15 mM in a phosphate buffer (50 mM, pH 7.5). For SANS measurements, the buffer was dissolved in D_2O (pH meter reading 7.0, corresponding to a pD of 7.4[22]). After five freeze–thaw cycles (liquid N_2, above 50 °C), the samples were extruded at 50 °C ten times through a membrane with 200 nm pores, followed by ten times through a membrane with 100 nm pores (Extruder from Lipex Biomembranes, Vancouver, Canada, and Nucleopore polycarbonate membranes from Sterico, Dietikon, Switzerland). Gelatin powder (5 and 10% (w/w)) was added to the bicellar solution and dissolved by gentle heating to about 50 °C.

Cryo-TEM. The samples were analyzed by cryo-transmission electron microscopy (cryo-TEM) following the procedure described previously.[23] Temperature was set to 40 °C in the VitrobotTM apparatus (FEI, Eindhoven, The Netherlands) before flash freezing by plunging into liquid ethane at the temperature of liquid nitrogen. The grids were examined at the temperature of liquid nitrogen using a cryo-holder (model 626, Gatan) and a Tecnai G2 F20 microscope (FEI) equipped with a field emission gun and Tridem energy filter (Gatan) operated at an accelerating voltage of 200 kV. The sample was observed at different tilting angles to gain additional information about the 3D structure. The data were recorded with 5–10 μm underfocus by using a 2048 × 2048 CCD camera (Gatan).

Rheological Measurements. A rheometer (Physica MCR501, Anton Paar) with a temperature controlled Couette geometry was used. The dynamic temperature sweep measurements were carried out from 50 to 5 °C with a heating and cooling rate of 1 °C/min at a constant shear strain amplitude γ = 10% and a constant angular frequency ω = 1 rad/s.

SANS. SANS measurements were performed on the SANS-I beamline at PSI, Villigen, Switzerland. The neutron wavelength was fixed at 8 Å, and data were collected using a two-dimensional ^{3}He detector at different distances covering a momentum transfer of $0.03 \leq q \leq 1.5$ nm^{-1}. Samples were placed during measurements inside a superconductive magnet with a horizontal field of up to 8 T perpendicular to the neutron beam. After correction for background radiation, empty cell scattering, and detector efficiency, the 2D intensity maps were radially averaged and fitted using the software package SASfit.[24] As form factor, a Porod's approximation for cylinder was used. To describe stacking, a structure factor for multilamellar structures was used, which accounts for thermal disorder caused by fluctuations of flat bilayers around well-defined and evenly spaced equilibrium positions.[25,26] An alignment factor A_f was extracted as a measure of the degree of orientation.[16]

DLS. Dynamic light scattering measurements were performed on a Malvern Zetasizer Nano ZS with noninvasive backscatter technology (NIBS) allowing the measurements of the undiluted bicellar samples. The sample was placed in a cuvette and illuminated at a fixed 90° angle with a He–Ne laser (623.8 nm).

Birefringence Measurements. Birefringence measurements were carried out on the basis of the phase modulation technique as described previously.[16,18]

RESULTS AND DISCUSSION

The motivation of the work was to investigate the possibility of integrating magnetically alignable bicelles into a hydrogel keeping the properties of the bicelles as well as of the gel. Cryo transmission electron microscopy (cryo-TEM), small angle neutron scattering (SANS), and birefringence measurements were performed with a focus on the effect of the applied magnetic field on the orientation of the embedded bicelles.

In a first step, the DPPC-based bicelles were investigated. Cryo-TEM micrographs of an aqueous mixture of DPPC/Chol/DPPE-DTPA/Tm^{3+} show the presence of bicelles and a few vesicles (see Figure 1). The flat structure of the bicellar aggregates was verified by taking cryo-TEM images at different tilting angles showing the same bicelle face-on (Figure 1A) and in a partial edge-on view (Figure 1B) in analogy to what has been found previously for DMPC/Chol/DMPE-DTPA/Tm^{3+} bicelles.[16] Some smaller bicelles are found in a complete edge-on view in Figure 1A.

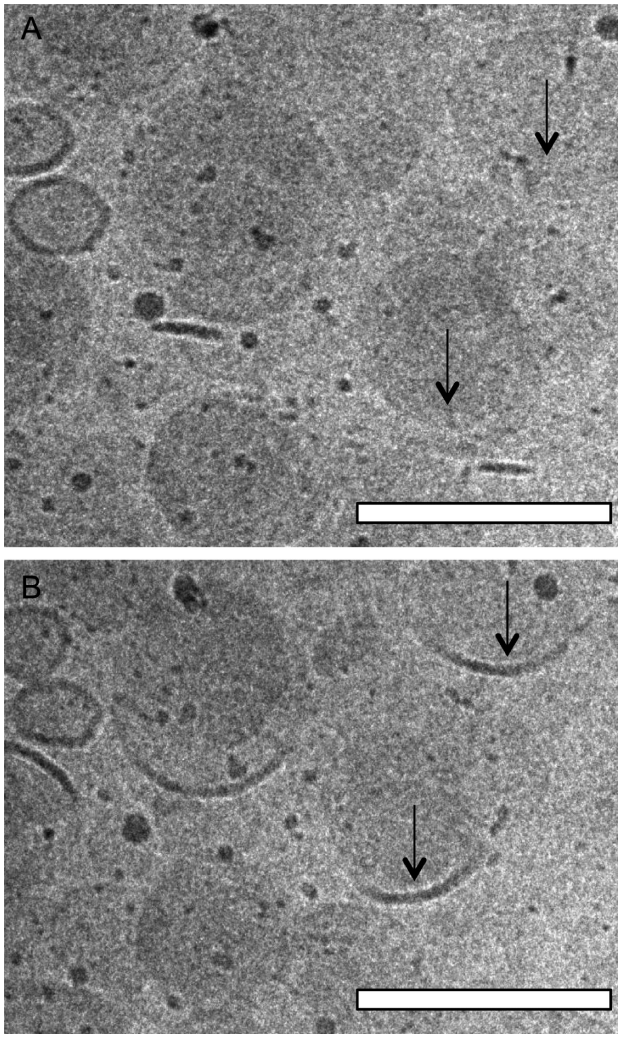

Figure 1. Cryo-TEM micrographs of an aqueous mixture of DPPC/Chol/DPPE-DTPA/Tm^{3+}, molar ratio of 16:4:5:5, and total lipid concentration of 15 mM, showing bicelles and a few vesicles. Image A was taken at 0° tilting angle, and image B was taken at a tilting angle of 30° around the horizontal axis (on the upper left of the two images). Arrows point to bicelles, which are in face-on view (A) and getting into edge-on view at the lower border (B). Scale bar = 200 nm.

In a next step, gelatin powder (5 and 10% (w/w), while only the 5% (w/w) will be considered in the following) was added to a bicellar solution and mixed at 50 °C, i.e., above the melting point of gelatin. Gelatin is a natural polymer forming a thermoreversible gel. Several studies of phospholipid vesicles in gelatin, collagen, or cross-linked gelatin matrices indicate the ability of these biopolmer gels to entrap phospholipid aggregates without destroying them.[27−32] We wondered if the same could be found for the bicelles we prepared. A 5% (w/w) gelatin solution was investigated with a rheological temperature sweep experiment at the relevant temperature rate of 1 °C/min, to determine the storage modulus G' and the loss modulus G''. The crossover of G' and G'' can be taken as an indication of the sol−gel transition point.[33] As shown in Figure 2, the gelling point upon cooling for the gelatin at a concentration of 5% (w/w) is around 22 °C, whereas the melting point is about 10 °C higher. The gelling point is lower than that reported in the literature (T_{gel} = 24−26 °C),[34,35] which is attributed to the fast temperature rate of 1 °C/min without equilibration time,

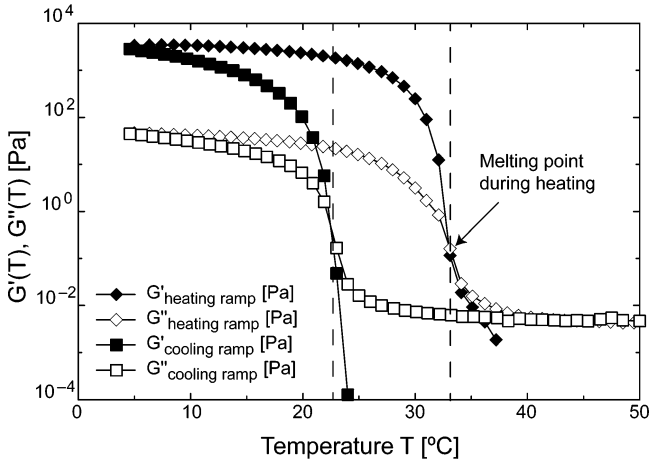

Figure 2. Storage modulus G' and loss modulus G'' of an aqueous gelatin solution (5% (w/w)) measured with a heating/cooling rate of 1 °C/min, γ = 10%, and ω = 1 rad/s. The gelling point is at 22 °C, and the melting point is at 33 °C, as determined from the crossover of the G' and G'' curves (indicated by dashed lines).

which we choose to represent the temperature profile of the SANS experiments. For the same reason, the hysteresis between cooling and heating is higher than the minimal hysteresis of 4 °C reported.[34]

SANS measurements were conducted to investigate first the influence of gelatin on the structure of the bicelles without applied magnetic field. The radially averaged curves of DPPC/Chol/DPPE-DTPA/Tm^{3+} without gelatin and embedded into 5% (w/w) gelatin at 40 °C and 0 T are shown in Figure 3, together with the scattering curve for gelatin alone.

The scattering of bicelles dominates over that from gelatin alone. DPPC/Chol/DPPE-DTPA/Tm^{3+} bicelles without gelatin was fitted well with a form factor for flat cylinders (i.e., disks) with a thickness d of 4.9 nm and a radius R of 80.2 nm.

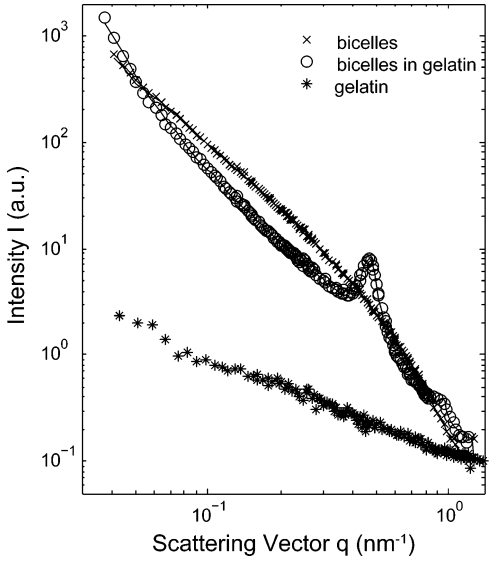

Figure 3. Radially averaged SANS curves and corresponding fit of DPPC/Chol/DPPE-DTPA/Tm^{3+} bicelles (molar ratio 16:4:5:5, total lipid concentration 15 mM) with and without gelatin 5% (w/w) and of gelatin only, measured at 40 °C and 0 T. The distinct peak found for bicelles embedded into the gelatin system is caused by stacking of the bicelles.

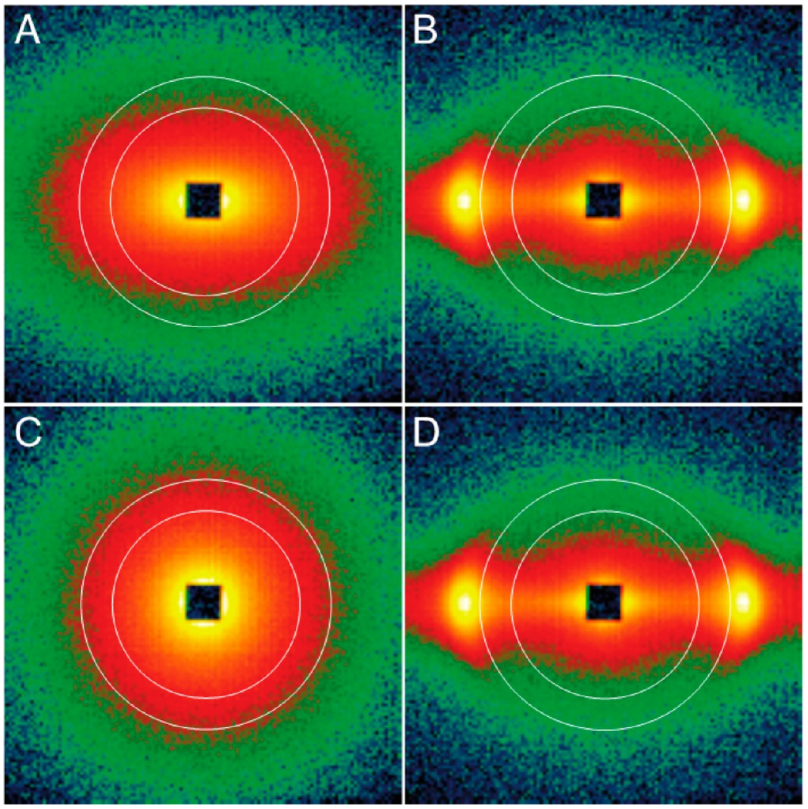

Figure 4. SANS 2D scattering pattern of DPPC/Chol/DPPE-DTPA/Tm^{3+} bicelles without (A,C) and with (B, D) gelatin measured at 5 °C. (A) and (B) are measured at 8 T and (C) and (D) after the magnet was ramped down to 0 T. Magnetic field direction is horizontal in the plane. White circles indicate the q-range used for the calculation of the alignment factors A_f, which are −0.2 (A), −0.6 (B), 0 (C), and −0.6 (D). Molar ratio of the bicellar mixtures was 16:4:5:5, total lipid concentration was 15 mM, and gelatin concentration was 5% (w/w).

The thickness is in good agreement with literature values on DPPC bilayers containing cholesterol.[36] The radius corresponds well with the hydrodynamic radius R_H = 82.5 nm measured with DLS at 40 °C. The fit of the bicelles embedded into the gelatin system consists of the same form factor as for flat cylinders (d = 4.9 nm, R = 80.2 nm) but includes in addition a structure factor for multilamellar structures accounting for a stacking of the bicelles. The parameters of the best fit are N = 4.7 for the stacking number, s = 13.2 nm for the stacking separation (disk to disk distance), and N_{diff} = 3.2 for the number of uncorrelated scattering bilayers. The structure factor comprises thermal disorder, caused by small fluctuations of the bilayers around well-defined mean layer positions; the Debye−Waller disorder parameter Δ for the best fit was 1.6. The stacking is most probably caused by thermodynamically driven depletion interaction between the bicelles and the gelatin molecules. The extent of stacking was not always the same for different samples and corresponding fits mainly differ in N_{diff}, the number of bicelles, which are not in a stack (data not shown).

SANS measurements of the same samples were also conducted inside a magnetic field of up to 8 T. 2D scattering patterns of DPPC/Chol/DPPE-DTPA/Tm^{3+} with and without gelatin, taken at 5 °C, 8 T, and a detector distance of 6 m, are shown in Figure 4A,B. The anisotropy of the scattering pattern indicates the aligning of the bicelles in the magnetic field with their disk normal parallel to the magnetic field direction. The anisotropy of the bicelles embedded into the gelatin system (Figure 4B) is more pronounced, most probably caused by stacking, thus increasing the aggregation number, which is proportional to the magnetic orientation energy.[37] The distinct peak in the direction of the magnetic field corresponds to the stacking distance, which is slightly shifted with temperature from 13.2 nm (40 °C) to 14.4 nm (5 °C). The scattering patterns after the magnetic field was ramped down to 0 T are shown in Figure 4C,D. Whereas the bicelles alone show an isotropic scattering, i.e., no orientation (Figure 4C), the bicelles embedded in gelatin keep their orientation even after removal of the magnetic field (Figure 4D).

The white circles in Figure 4 indicate the q-range, which was used for the calculation of the alignment factor A_f. For increasing anisotropy of the scattering pattern, the modulus of A_f gets larger, indicating a higher degree of orientation of the bicelles. A positive A_f value corresponds to scattering perpendicular to the magnetic field direction, negative to parallel orientation, respectively. This factor is plotted in Figure 5 as a function of the magnetic field for DPPC/Chol/DPPE-DTPA/Tm^{3+} bicelles at 40 and 5 °C with and without gelatin. In measurements without gelatin, the aligning of the bicelles increases with increasing magnetic field strength, without reaching any saturation (see Figure 5). The most pronounced alignment was found at the lowest temperature (5 °C), which is in agreement with previous studies on DMPC/Chol/DMPE-DTPA/Tm^{3+} bicelles.[16]

The alignment at 40 °C is increased if the bicelles are embedded into gelatin, which is due to disk stacking, as discussed above (see Figure 4). The A_f curve of bicelles in gelatin at 40 °C has a sigmoidal shape, indicating that the orientation almost reaches saturation. If the sample is cooled at 8 T to 5 °C, the sample keeps its orientation, even if the

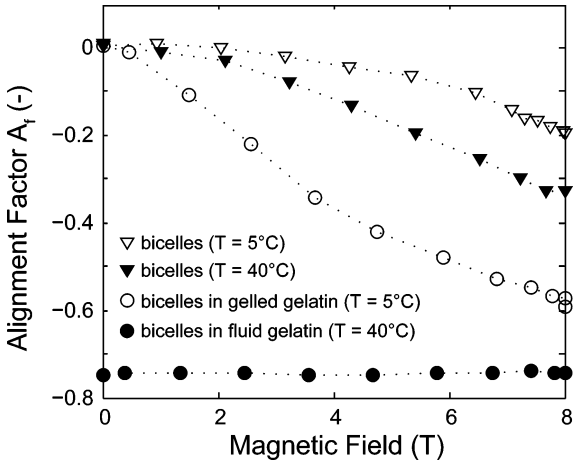

Figure 5. Alignment factor as a function of the magnetic field strength of DPPC/Chol/DPPE-DTPA/Tm^{3+} (molar ratio of 16:4:5:5, total lipid concentration of 15 mM) embedded in gelatin (5% w/w) and without gelatin at 40 and 5 °C. Cooling from 40 to 5 °C is performed with an applied field of 8 T.

magnetic field is ramped down (see Figure 5). A_f stays constant from 8 to 0 T, showing the capability of gelatin to entirely fix the orientation of bicelles.

The temperature dependence of the alignment of DPPC/Chol/DPPE-DTPA/Tm^{3+} bicelles with and without gelatin is shown in Figure 6. If the bicelles are cooled at 8 T, the

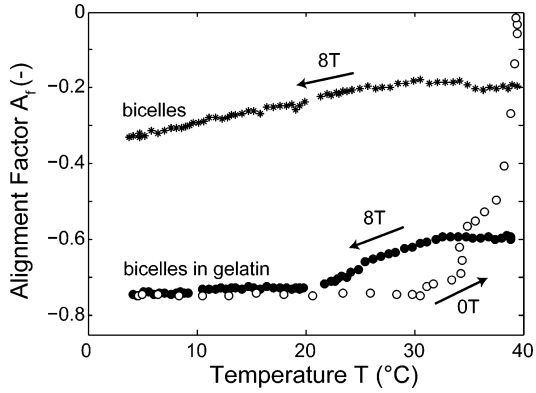

Figure 6. Alignment factor as a function of temperature of bicelles (DPPC/Chol/DPPE-DTPA/Tm^{3+} 16:4:5:5, lipid concentration of 15 mM) with and without gelatin (5% w/w). During cooling, a magnetic field of 8 T was applied; heating up was performed without magnetic field applied.

alignment factor decreases slightly, indicating a pronounced orientation with decreasing temperature. If the bicelles are embedded into the gelatin system, A_f decreases with decreasing temperature from 40 to 20 °C but is constant if the temperature is lowered further. Similar alignment profiles as shown in Figure 6 are obtained for gelatin concentrations of 10% (w/w), while for gelatin concentration below 5% (w/w) only a partial gelation and, thus, a limited fixation of the bicelles was observed (data not shown).

This coincides with the gelation point of gelatin, which is around 22 °C for this cooling rate as determined with rheological measurements (Figure 2). Most interestingly, however, if the sample is heated after switching off the magnetic field (open circles in Figure 6), the alignment remains fairly constant until about 30 °C (the melting point of gelatin, Figure 2), where the bicelles start to deorientate until the alignment factor reaches 0 (isotropic scattering pattern). The stepwise deorientation seen in Figure 6 (B = 0 T, empty circles) between 31 and 38 °C is attributed to the stepwise temperature regulation in the bore of the superconducting magnet and was not observed in SANS experiment performed outside the magnet (data not shown).

With regard to a possible application of such bicelle containing macrostructure as a new smart material, we were interested in studying its anisotropy for electromagnetic wave transmission. Therefore, birefringence measurements were carried out on DPPC/Chol/DPPE-DTPA complexed with either Tm^{3+} or Dy^{3+}, which were gelled inside a magnetic field of 5.5 T and measured after removal of the field in all three spatial directions. Tm^{3+} induces orientation of the bicellar normal parallel to the magnetic field as shown previously.[18] Complexation of Dy^{3+}, however, results in an orientation of the bicellar normal perpendicular to the magnetic field, as schematically shown in Figure 7. A background birefringence

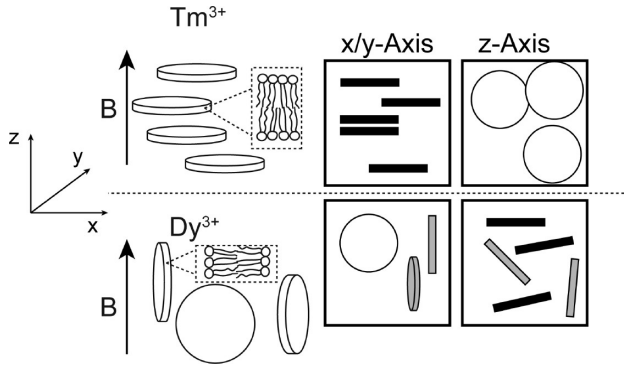

Figure 7. Schematic view of bicelles orienting in magnetic field complexed with Tm^{3+} (top) and Dy^{3+} (bottom). Shading indicates the birefringence signal measured in the different spatial orientations, with black for positive, gray for negative birefringence, and white for no birefringence.

of 1.5×10^{-7} was detected for gelatin alone. For samples with Tm^{3+}, the signal in the direction of the x- and y-axis was an order of magnitude larger, with 4.0×10^{-6}, whereas the value in z-axis was close to the background signal (2.0×10^{-7}). For the sample with Dy^{3+}, the value measured in the direction of the x/y-axis was a large negative value (-3.7×10^{-6}), whereas the z-axis was again close to the background signal (3.5×10^{-7}). No significant change of the birefringence signal compared to the background was observed for the control, which was gelled without applied magnetic field. The measured values are consistent with the theoretically expected birefringence values of oriented bicellar samples, as indicated in Figure 7 (right). The optical axis of a phospholipid molecule is equal to the long molecular axis, i.e., parallel to its fatty acid tails,[38] thus, no birefringence is observed if measured in the direction of the long molecular axis. This is the case of bicelles with complexed Tm^{3+} measured in the direction of the z-axis (face-on view of bicelles, indicated with white circles).

If the birefringence is measured in the direction of the y-axis, the molecules doped with Tm^{3+}, consequently aligned in the z-direction, show a positive birefringence value (bicelles in edge-on view, black). Molecules with Dy^{3+} aligning with their long-molecular axis perpendicular to the magnetic field can still

dx.doi.org/10.1021/am4046469 | ACS Appl. Mater. Interfaces 2014, 6, 1100−1105

rotate around the magnetic field axis. Thus, in their extreme, positions will be oriented either in the direction of the *x*-axis, showing a negative birefringence value (bicelles in edge-on view, gray), or in the direction of *y*-axis, thus showing no birefringence (bicelles in face-on view, white) if measured in the *x*/*y*-axis. Measured in the *z*-axis, Dy^{3+} bicelles are found face-on in all possible directions (positive and negative birefringence values); thus, the birefringence is canceled out.

CONCLUSION

In this report, we show that the magnetic aligning of bicelles formed by a mixture of DPPC/Chol/DPPE-DTPA/Tm^{3+} can be fixed with the addition of 5% (w/w) of gelatin. Bicelles in the gelatin system are partially stacked, most probably caused by thermodynamically driven depletion interaction between the bicelles and the gelatin molecules. This stacking leads to an increase of the alignability compared to the same bicelles in aqueous mixtures. This is due to the conjunct movement of the stacks; thus, the aggregation number, which is proportional to the magnetic orientation energy, is increased. If a mixture of bicelles and gelatin is cooled down in a magnetic field, its alignment increases until about 20 °C, the gelling point of gelatin, remaining constant if the sample is cooled even further. As shown with SANS measurements, the alignment stays unchanged after removal of the magnetic field until up to about 30 °C, which is the melting point of gelatin. The sample gelled under magnetic field shows an anisotropic birefringence even after removal of the applied magnetic field. All results are in agreement with a successful fixation of the magnetic field orientation of the bicelles by gelatin.

AUTHOR INFORMATION

Corresponding Author

*E-mail: peter.fischer@hest.ethz.ch.

Notes

The authors declare no competing financial interest.

ACKNOWLEDGMENTS

The authors acknowledge EMEZ for technical support and S. Bolisetty for assistance during DLS measurements. This work is based on experiments performed at the Swiss spallation neutron source SINQ, Paul Scherrer Institute, Villigen, Switzerland. The Swiss National Foundation is acknowledged for funding (Project number 200021_132132).

REFERENCES

(1) Gil, E. S.; Hudson, S. M. *Prog. Polym. Sci.* **2004**, *29*, 1173−1222.
(2) Kumar, A.; Srivastava, A.; Galaev, I. Y.; Mattiasson, B. *Prog. Polym. Sci.* **2007**, *32*, 1205−1237.
(3) Liu, T.-Y.; Hu, S.-H.; Liu, D.-M.; Chen, S.-Y.; Chen, I. W. *Nano Today* **2009**, *4*, 52−65.
(4) Satarkar, N. S.; Biswal, D.; Hilt, J. Z. *Soft Matter* **2010**, *6*, 2364−2371.
(5) Vermonden, T.; Censi, R.; Hennink, W. E. *Chem. Rev.* **2012**, *112*, 2853−2888.
(6) Ghosh, S.; Cai, T. *J. Phys. D: Appl. Phys.* **2010**, *43*, 415504.
(7) Liu, T.-Y.; Hu, S.-H.; Liu, K.-H.; Liu, D.-M.; Chen, S.-Y. *J. Controlled Release* **2008**, *126*, 228−236.
(8) Reinicke, S.; Dohler, S.; Tea, S.; Krekhova, M.; Messing, R.; Schmidt, A. M.; Schmalz, H. *Soft Matter* **2010**, *6*, 2760−2773.
(9) Zrínyi, M. *Colloid Polym. Sci.* **2000**, *278*, 98−103.
(10) Momota, H.; Yokoi, H.; Takamasu, T. *J. Nanosci. Nanotechnol.* **2010**, *10*, 3849−3853.
(11) Christianen, P. C. M.; Shklyarevskiy, I. O.; Boamfa, M. I.; Maan, J. C. *Phys. B: Condens. Matter* **2004**, *346*−*347*, 255−261.
(12) Shklyarevskiy, I. O.; Jonkheijm, P.; Christianen, P. C. M.; Schenning, A.; Meijer, E. W.; Henze, O.; Kilbinger, A. F. M.; Feast, W. J.; Del Guerzo, A.; Desvergne, J. P.; Maan, J. C. *J. Am. Chem. Soc.* **2005**, *127*, 1112−1113.
(13) Binnemans, K.; Gorller-Walrand, C. *Chem. Rev.* **2002**, *102*, 2303−2345.
(14) Prosser, R. S.; Volkov, V. B.; Shiyanovskaya, I. V. *Biophys. J.* **1998**, *75*, 2163−2169.
(15) Beck, P.; Liebi, M.; Kohlbrecher, J.; Ishikawa, T.; Rüegger, H.; Fischer, P.; Walde, P.; Windhab, E. J. *Langmuir* **2010**, *26*, 5382−5387.
(16) Liebi, M.; Kohlbrecher, J.; Ishikawa, T.; Fischer, P.; Walde, P.; Windhab, E. J. *Langmuir* **2012**, *28*, 10905−10915.
(17) Liebi, M.; Kuster, S.; Kohlbrecher, J.; Ishikawa, T.; Fischer, P.; Walde, P.; Windhab, E. J. *J. Phys. Chem. B* **2013**, *117*, 14743−14748.
(18) Liebi, M.; van Rhee, P. G.; Christianen, P. C. M.; Kohlbrecher, J.; Fischer, P.; Walde, P.; Windhab, E. J. *Langmuir* **2013**, *29*, 3467−3473.
(19) Koynova, R.; Caffrey, M. *Biochim. Biophys. Acta* **1998**, *1376*, 91−145.
(20) Fischer, P. *Eur. Phys. J. Spec. Top.* **2013**, *222*, 73−81.
(21) Aikawa, K.; Nishigaki, J.; Takahashi, K. Glycerophosphoric acid ester derivate having polyfunctional metal chelate structure. EP1795208A1, 2007−06−13.
(22) Covington, A. K.; Paabo, M.; Robinson, R. A.; Bates, R. G. *Anal. Chem.* **1968**, *40*, 700−706.
(23) Ishikawa, T.; Sakakibara, H.; Oiwa, K. *J. Mol. Biol.* **2007**, *368*, 1249−1258.
(24) Kohlbrecher, J. Software package SASfit for fitting small-angle scattering curves. http://kur.web.psi.ch/sans1/SANSSoft/sasfit.html (accessed February 11, 2013).
(25) Frühwirth, T.; Fritz, G.; Freiberger, N.; Glatter, O. *J. Appl. Crystallogr.* **2004**, *37*, 703−710.
(26) Pabst, G.; Koschuch, R.; Pozo-Navas, B.; Rappolt, M.; Lohner, K.; Laggner, P. *J. Appl. Crystallogr.* **2003**, *36*, 1378−1388.
(27) DiTizio, V.; Ferguson, G. W.; Mittelman, M. W.; Khoury, A. E.; Bruce, A. W.; DiCosmo, F. *Biomaterials* **1998**, *19*, 1877−1884.
(28) DiTizio, V.; Karlgard, C.; Lilge, L.; Khoury, A. E.; Mittelman, M. W.; DiCosmo, F. *J. Biomed. Mater. Res.* **2000**, *51*, 96−106.
(29) Dowling, M. B.; Lee, J.-H.; Raghavan, S. R. *Langmuir* **2009**, *25*, 8519−8525.
(30) Madhavarao, C. N.; Sauna, Z. E.; Sitaramam, V. *Biophys. Chem.* **2001**, *90*, 147−156.
(31) Peptu, C.; Popa, M.; Antimisiaris, S. G. *J. Nanosci. Nanotechnol.* **2008**, *8*, 2249−2258.
(32) Weiner, A. L.; Carpenter-Green, S. S.; Soehngen, E. C.; Lenk, R. P.; Popescu, M. C. *J. Pharm. Sci.* **1985**, *74*, 922−925.
(33) Winter, H. H.; Chambon, F. *J. Rheol.* **1986**, *30*, 367−382.
(34) Brand, T.; Richter, S.; Berger, S. *J. Phys. Chem. B* **2006**, *110*, 15853−15857.
(35) Matsunaga, T.; Shibayama, M. *Phys. Rev. E* **2007**, *76*, 030401.
(36) Reinl, H.; Brumm, T.; Bayerl, T. M. *Biophys. J.* **1992**, *61*, 1025−1035.
(37) Qiu, X. X.; Mirau, P. A.; Pidgeon, C. *Biochim. Biophys. Acta* **1993**, *1147*, 59−72.
(38) Lee, C. W.; Decca, R. S.; Wassall, S. R.; Breen, J. J. *Phys. Rev. E* **2003**, *67*, 061914.